

Field and laboratory assessment of ground subsidence induced by underground cavity under the sewer pipe

Suk-Min Kong^{1a}, Dong-Min Kim^{2b}, Dae-Young Lee^{2c}, Hyuk-Sang Jung^{3d} and Yong-Joo Lee^{*1}

¹Department of Civil Engineering, Seoul National University of Science and Technology,
232 Gongneung-ro, Nowon-gu, Seoul 01811, Korea

²Geotechnical Engineering Research Division, Korea Institute of Civil Engineering and Building Technology,
283, Goyang-daero, Ilsanseo-gu, Goyang-si, Gyeonggi-do, 10223, Korea

³Department of Railroad Construction and Safety Engineering, Dongyang University,
145 Dongyangdaero, Punggi, Yeongju, Gyeongbuk, 750-711, Korea

(Received January 8, 2018, Revised May 21, 2018, Accepted June 19, 2018)

Abstract. In densely populated urban areas with a large amount of infrastructure, ground subsidence events can result in massive casualties and economic losses. In South Korea, the incidence of ground subsidence in urban areas has increased in recent years and the number of underground cavities suspected of causing such events has significantly increased. Therefore, it is essential to develop techniques to prevent the occurrence of underground and ground subsidence. In this study, a field test, laboratory test, and numerical analysis were conducted to determine the optimal compaction degree of the upper support layer of any underground cavity below the level of sewer pipes in order to prevent such cavities from collapsing and leading to ground subsidence accidents. During the field test, an underground cavity was simulated using ice, and the generation of the cavity was confirmed using ground penetrating radar. The ground investigation was performed using a cone penetration test, and the compaction of the ground where ground subsidence occurred was evaluated with a laboratory test. The behaviour of the ground under various conditions was predicted using a numerical analysis based on the data obtained from the field test and previous studies. Based on these results, the optimal compaction degree of the ground required to prevent the underground cavity from causing ground subsidence was predicted and presented.

Keywords: ground subsidence; compaction; CPT; field test; laboratory test; numerical analysis

1. Introduction

The incidence of underground cavities and ground subsidence has been increasing recently due to climate change, urban development, and the aging of facilities, such as sewer pipelines, and there has been increasing domestic and overseas interest in such events. In 2010, a ground subsidence of 20 m in diameter and 30 m in depth occurred in Guatemala City, which resulted in the collapse of a three-story factory and the death of 15 people. Upon investigation, it was found that this event was caused by a poor drainage system and the loss of soil due to water flowing out of an old broken drain pipe (Park and Park 2014). A 15-m-wide ground subsidence even later occurred in Fukuoka city center in 2015. Ground subsidence

problems continue to occur in many countries globally. In South Korea in 2016, 85 cases of ground subsidence and 803 cases of ground settlement occurred in Seoul alone, which was an increase of 51% and 9.4%, respectively, compared to 2015. Researchers in Seoul city explored 1,114 km of street underground space and identified 515 underground cavities, most of which were located where there were a number of the underground utilities and excavation restorations. While ground settlement due to consolidation occurs over a continuous range at low speed and thus allows some time to establish countermeasures, upper layer subsidence caused by underground cavities is fast and discontinuous and often results in the loss of lives and property damage (Im 2015).

The most cause of ground subsidence is caused by underground cavities. The underground cavity is occurred by causes of natural and anthropogenic. First, in nature, the limestone cavity is made by the chemical reaction between groundwater and limestone (Fig. 1). The underground cavity is formed by molten limestone and leads to the sinkhole (Tihansky 1999, Perez *et al.* 2017). Next, cause of anthropogenic is classified into two kinds. The first is drainage accompanied by the discharge of soil particles and poor backfilling during underground excavation, while the second is the discharge of soil particles along with sewage when old sewer pipes are damaged (Fig. 2). In South Korea, 80% of ground subsidence events are caused by old and

*Corresponding author, Professor

E-mail: ucesyjl@seoultech.ac.kr

^aPh.D. Student

E-mail: sukminik@naver.com

^bResearcher

E-mail: dmkim@kict.re.kr

^cResearch fellow

E-mail: dylee@kict.re.kr

^dProfessor

E-mail: yoricom@dyu.ac.kr

damaged sewer pipes. Old sewer pipes in need of emergency repairs in Seoul represent almost 16% of all sewer pipes, while 40% require only general repairs (Oh *et al.* 2015).

Kuwano *et al.* (2010) studied the patterns of the ground behaviours and relaxation zone using a laboratory model test system capable of supplying and discharging water, the particle image velocimetry (PIV) technique, and computer tomography (CT) imaging. For sandy ground, a large relaxation zone with a 15% decrease in density progressed rapidly. In contrast, for clay ground, a small relaxation zone with a 50% decrease in density progressed relatively slowly, and larger cavities were observed than those in the sandy ground. In addition, Sato and Kuwano (2015) conducted a laboratory model test to investigate the effects of underground cavities resulting from sewer pipe breakage on underground structures and the area distribution of loose zones where the strength decreased due to ground subsidence. In contrast to the research by Sato and Kuwano (2015), this research has focused on the subsurface cavity developed just below the sewer pipe.

Oh *et al.* (2016) simulated a damaged sewer pipe using a laboratory model test. They studied the ground surface settlement caused by the soil discharged due to the sewer pipe breakage and the corresponding impact range using different relative densities of loose ground (relative density 30%) and dense ground (relative density 70%). Little ground surface settlement was observed to occur in dense ground conditions. On the other hand, in the case of the loose ground, a ground surface settlement of 115 mm occurred and a 215-mm deep depression formed below the lower part of the pipe. To complement existing techniques for investigating underground cavities, laser scanning methods are in development to rapidly detect and accurately measure the dimensions of underground cavities (Cui *et al.*, 2017).

In addition, Lee (2015) developed a backfill material that can prevent the breakage of sewer pipes and ground settlement by supporting the overburden load in case of an underground cavity. This material was tested with an artificial underground cavity constructed using an ice block around a sewer pipeline. A field test was performed to compare the benefits of using the developed backfill material versus conventional sand compaction. When the developed backfill material was used, the maximum cross section and longitudinal section of the ground settlement were 23.4 cm and 27 cm, respectively, while in the case of the sand compaction, there was no change in the ground settlement amount.

In this study, the underground cavity caused by the old sewer pipe was simulated using an ice block. After the ice melted, the ground surface settlement amount was observed and the cone penetration resistance (q_c) value of the ground versus the depth was measured using a cone penetration test. In the laboratory test, ground with various relative densities was created by applying different compaction times for each case. The correlation between the q_c value and relative density was plotted using a cone penetration test. In addition, various ground behaviours were predicted through numerical analysis. In the case of an underground cavity, the optimal compaction degree that did not lead to immediate ground subsidence was estimated by comparing the laboratory test results with the field test data.

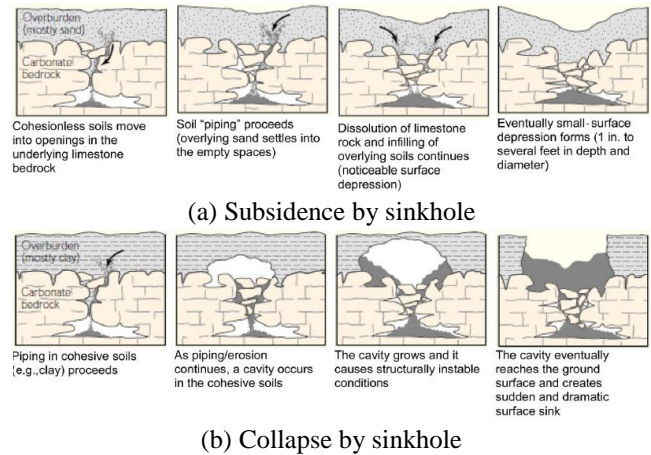


Fig. 1 Major sinkhole types (Tihansky 1999)

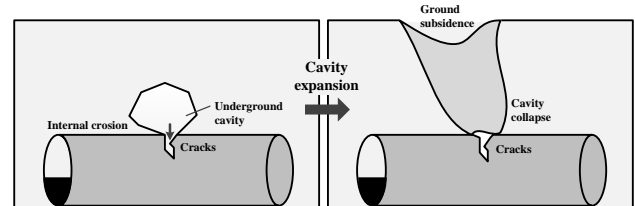


Fig. 2 Underground cavity caused by the sewer pipe (Sato and Kuwano 2015)

2. Field test

2.1 Field test conditions

A field test was conducted at a site located in Namyangju where the landfill layer extended to 3 m below the surface to simulate underground cavities caused by sewage leakage, loss of the surrounding ground, and the subsequent ground settlement resulting from a break in a sewer pipe due to age or external factors. A sewer pipe with a diameter of 450 mm and length of 2,500 mm was installed at a 1 m depth (Fig. 3), and site compaction was performed through sand compaction. A 3,500 × 1,000 × 250 mm ice block was buried below the sewer pipe, as shown in Fig. 4, which resulted in an artificial underground cavity once the ice melted. The melting of the ice block and the creation of the underground cavity was confirmed using ground penetrating radar (GPR) (Fig. 5). Before the ice block melted, the q_c value of the ground was measured with a cone penetration test (Fig. 6) in which a penetration cone with a $\Phi 16$ mm and a 30° point angle was used and corrected using a standard instrument that maintained traceability in SI units from the Korea Research Institute of Standards and Science (KRISS). Cone penetration test measurements were performed the four positions shown in Fig. 7. A schematic of the field test is shown in Fig. 8.

2.2 Field test results

GPR (Ground Penetration Radar) is the most commonly used method for investigating underground in urban areas due to user convenience and cost effective (Kim *et al.* 2000, Ryu *et al.* 2015). So, in this test, GPR is used to find



Fig. 3 Field test pipe installation



Fig. 4 Ice block

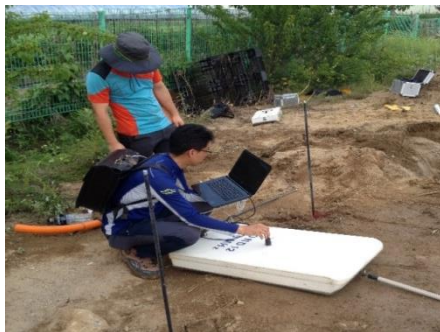


Fig. 5 GPR test



Fig. 6 Field cone penetration test

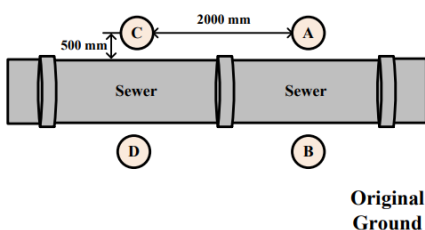


Fig. 7 Measurement position plan view

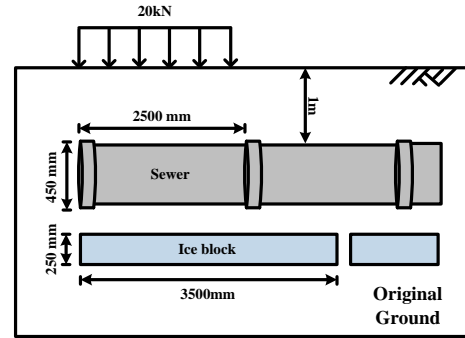
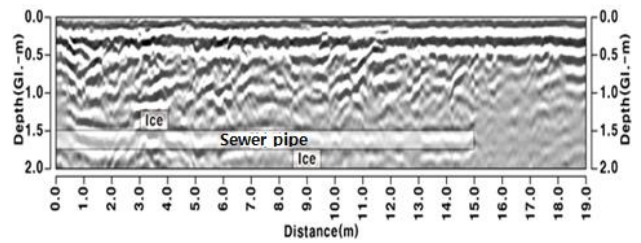
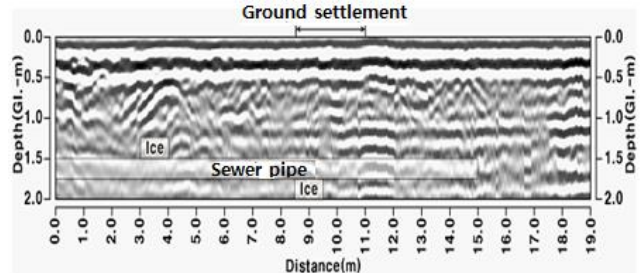


Fig. 8 Field test sectional view



(a) 1st days after the field test was completed



(b) 15th days after the field test was completed

Fig. 9 GPR observation results

underground cavity. The GPR detection analysis results are shown in Fig. 9. While detecting cavities around the sewer pipe at a 1.5 m depth using a frequency of 300 MHz, a parabolic reflection surface was detected at the top of the sewer pipe. This appears to be a reflection surface caused by a cavity that formed at the top of the sewer pipe as the ice melted. A GPR survey was conducted on the 1st, 5th, and 15th days after the field test, and larger parabolic reflections were detected on the 5th and 15th days than that immediately after the installation. It is believed that the cavity above the pipe was enlarged as the ice melted. In contrast, no reflection surface was observed at the position where ice was buried under the sewer pipe, although this was likely due to the fact that the radar wave did not extend under the sewer pipe.

The measurements of the cone penetration test conducted before the melting ice blocks generated the underground cavities are shown in Fig. 10. Cone penetration test measurements at depths up to 500 mm were possible at measurement positions A, B, and D, but only up to 100 mm at position C. It was estimated from the maximum cone penetration depth and q_c value of each position that the compaction at measurement position C was the highest relative to that at the other positions, and the compaction at measurement position D was the loosest. The

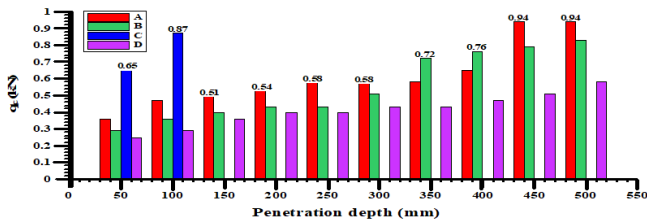


Fig. 10 Cone penetration test results



(a) Ground subsidence at position C



(b) Ground subsidence at position D



(c) Ground subsidence at position D

Fig. 11 Observations of the ground subsidence

observation results three days after the site construction are shown in Fig. 11. Once the ice was sufficiently melted, the presence of ground settlement at measurement positions A, B, and D was visually confirmed. The settlement at position D was measured to be more than 140 mm, as shown in Fig. 11(c). In contrast, the settlement at position C was found to be less than 10 mm.

3. Laboratory test

3.1 Compaction test

In the laboratory test, an initial experiment was

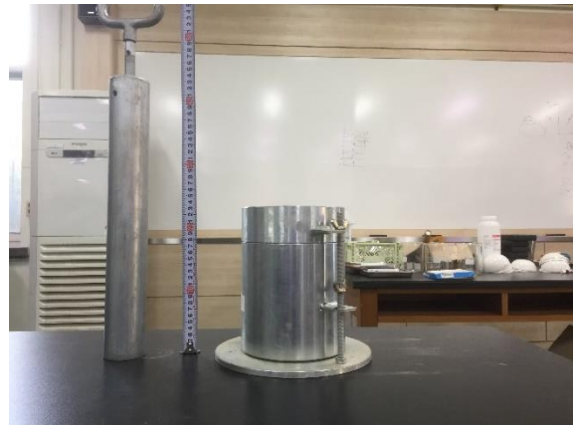


Fig. 12 Laboratory compaction test with standard mold

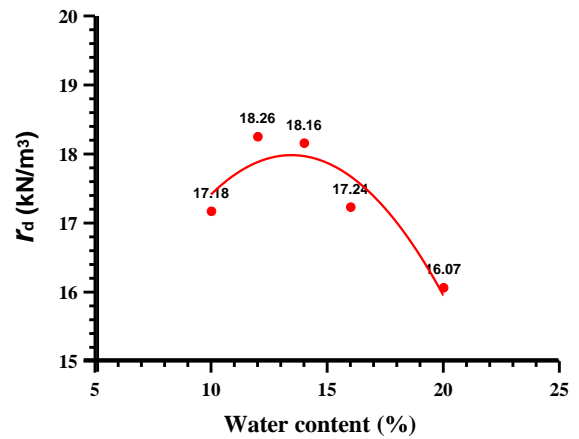


Fig. 13 Dry density–water content curve



Fig. 14 Fabricated mold and rammer

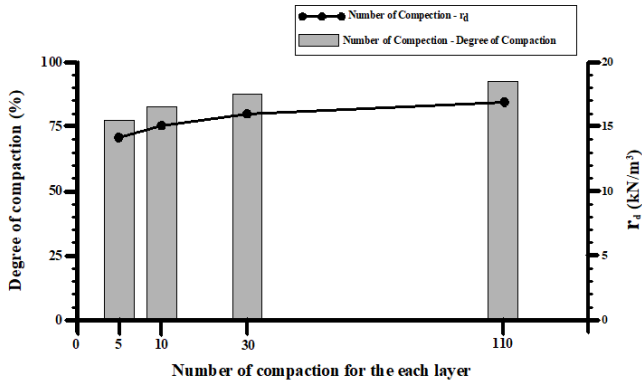


Fig. 15 Number of compactions vs. compaction degree vs. dry unit weight

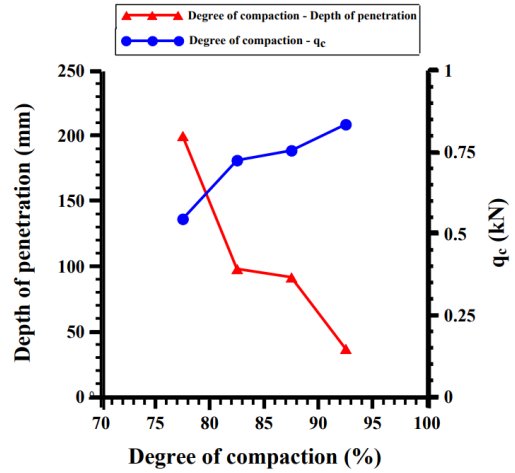
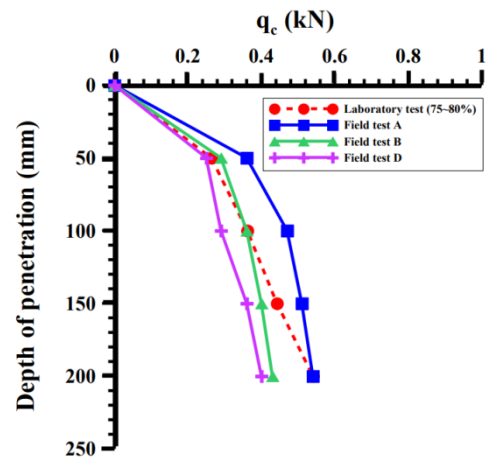


Fig. 16 Compaction degree-penetration depth- q_c

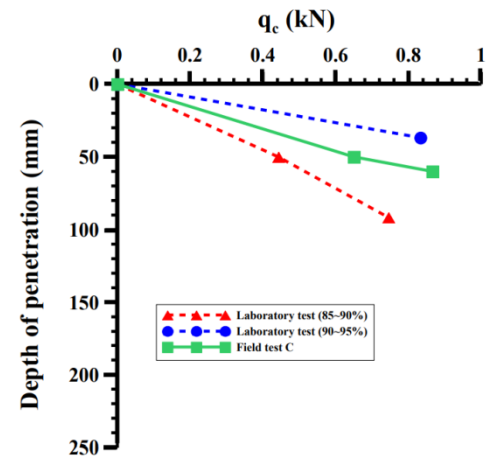
conducted to determine the maximum and minimum dry compaction weight of the soil using the drying and non-repeating methods. A rammer with a 2.5 kg weight and a mold with a 15-cm inner diameter and a height of 20 cm height were used (Fig. 12). The test methods and studies described in Lambe and Whitman (1979) and Lee *et al.* (2007) were adopted. The dry density-water content curve is shown in Fig. 13. In this study, the maximum dry unit weight of the soil was calculated to be 18.26 kN/m³ according to the dry density-water content curve using a water content of 12%. To obtain the minimum dry unit weight, the soil was loosely poured into a mold through a tube with a 12.7 mm diameter and a funnel at the end, and the drop height was maintained at 25.4 mm. The minimum dry unit weight of the site was measured to be 12.62 kN/m³ according to the ratio of the volume to the weight of the soil (Das 2009). In the laboratory compaction test to estimate the compaction of the site, a 5.0 kg rammer applied according to the double similarity law and the B compaction method along with a mold with an inner diameter of 30 cm and a height of 40 cm (Fig. 14). When investigating the compaction degree according to the number of compactions, a total of six sets of compaction tests were conducted with 110, 80, 30, 10, 5, and 0 compaction repetitions per layer for three compaction layers. Four additional compaction tests were performed for the cases that exhibited compaction degrees of 95-90%, 90-85%, 85-80%, and 80-75%. Once the tests were completed, the mean values of a total of five compaction tests were obtained (Fig. 15).

3.2 Cone penetration test

Cone penetration tests are commonly used for investigating the characteristics of ground, and a portable cone penetration tester can perform tests easily and economically in a short period of time (Kim *et al.* 2017, Mouna *et al.* 2017, Zein 2017). During the field test, quick tests were conducted using a portable cone penetration tester before the ice block melted. In the laboratory test, a cone penetration test was conducted on the ground prepared by the previous compaction test using the same tester, and the penetration depth and q_c value according to the compaction degree were measured. The cone penetration



(a) Field A, B, D vs. a laboratory test compaction degree of 75-80%



(b) Field C vs. a laboratory test compaction degree of 85-95%

Fig. 17 Comparison between the field and laboratory tests

test was conducted in a total of five directions, which were the mold center, and the 12 o'clock, 3 o'clock, 6 o'clock, and 9 o'clock directions, for each degree of compaction to obtain mean values. In the cases where the degree of compaction was 75-80%, the penetration depth was only measured up to 20 cm due to the height limit of the mold

employed in the laboratory test. As the degree of compaction increased, the penetration depth decreased. Fig. 16 shows the plotted correlation among the compaction degree, penetration depth of the laboratory cone penetration test, and q_c value for each case, which were obtained through the compaction test. It was found that the q_c value increased as the degree of compaction increased. For comparison purposes, Fig. 17 depicts the results of the field cone penetration test along with those of the laboratory cone penetration test. After estimating the compaction degree of the site using the laboratory test results, it was determined that the compaction degree was approximately 75-80% at measurement positions A, B, and D, while at measurement position C, the compaction degree was estimated to be more than 85%. Based on the results of this study, it was observed that the ground surface did not collapse easily even when there was an underground cavity when the compaction degree of the site was more than 85%. On the other hand, when the compaction degree was less than 80%, ground surface settlement did occur. Therefore, it is desirable to ensure the degree of compaction of sites is higher than 85%.

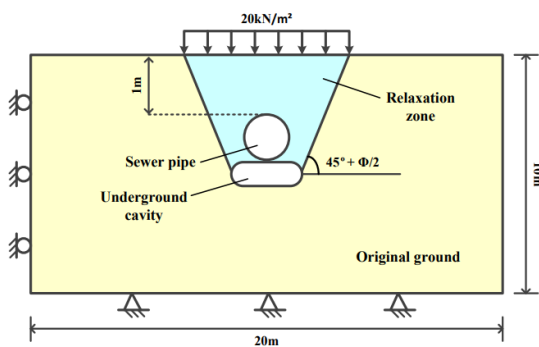
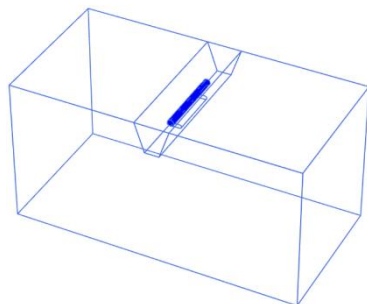
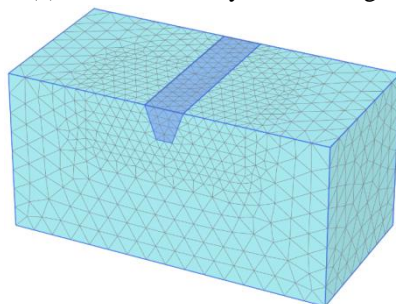


Fig. 18 Numerical analysis sectional view



(a) Numerical analysis modeling



(b) Numerical analysis mesh

Fig. 19 3D numerical analysis

Table 1 Material properties for numerical analysis

Parameters	Loose		Dense		Sewer pipe
	Original ground	Relaxation zone	Original ground	Relaxation zone	
γ (kN/m ³)	14.2	12.1	17.0	14.5	23.0
e	0.72	0.83	0.63	0.72	-
E (kN/m ²)	3,000	2,550	10,000	8,500	2.45×10^7
ν	0.2	0.2	0.3	0.3	0.3
c (kN/m ²)	0.7	0.6	2.3	2.0	-
Φ' (°)	27	23	35	30	-
d (m)	-	-	-	-	0.45

γ : Unit weight of soil, e : Void ratio, E : Young's modulus, ν : Poisson's ratio, c : Cohesion, Φ' : Internal friction angle, d : Diameter of sewer pipe

4. Numerical analysis

4.1 Numerical analysis conditions

The Plaxis 3D (2016) software package was used for the numerical analysis in this study. In the simulation, the dimensions of the target ground were $20,000 \times 10,000 \times 10,000$ mm, and the sizes and positions of the sewer pipe and underground cavity were simulated under the same conditions as in the field test (Fig. 18). The numerical analysis modeling and mesh are shown in Fig. 19, and the material properties used in the numerical analysis were based on the data from the laboratory test and that obtained by Ham (2009). A numerical analysis was conducted for weathered soil with compaction degrees of 75% and 90%. In addition, in terms of the material properties of the relaxation zone caused by an underground cavity, a 15% lower density compared to that of the existing ground was applied by referring to the study of Kuwano *et al.* (2010). It was assumed that the relaxation zone proceeded from an underground cavity in the $(45^\circ + \Phi/2)$ direction. The ground construction model was based on the Mohr-Coulomb model, and an elastic model was used to model the sewer pipe. Table 1 shows the material properties of the ground and sewer pipe used in the numerical analysis.

4.2 Numerical analysis results

The ground displacement vector caused by the occurrence of an underground cavity is shown in Fig. 20. In the loose ground condition, the ground around the sewer pipe totally collapsed due to the underground cavity. On the other hand, a slight displacement occurred in the underground cavity in the case of dense ground, although it did not significantly affect the surrounding ground. As shown Fig. 21, a similar tendency appeared in the vertical displacement. While a vertical displacement in the loose ground occurred over the entire relaxation zone due to the large vertical displacement in the underground cavity, the vertical displacement in the dense ground occurred only in the vicinity of the underground cavity. In the case of the loose ground, a maximum of 148 mm ground surface settlement occurred immediately above the underground

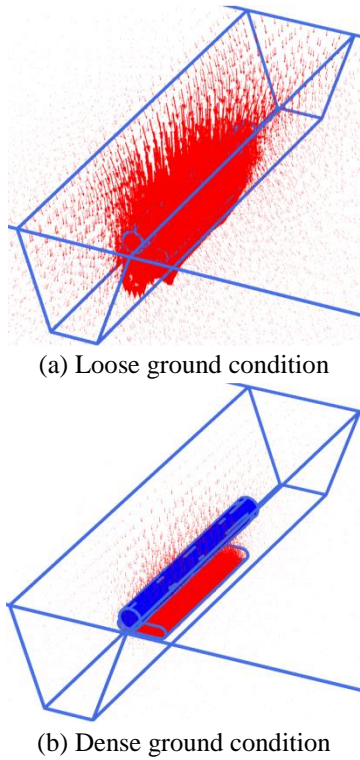


Fig. 20 Total displacement vectors

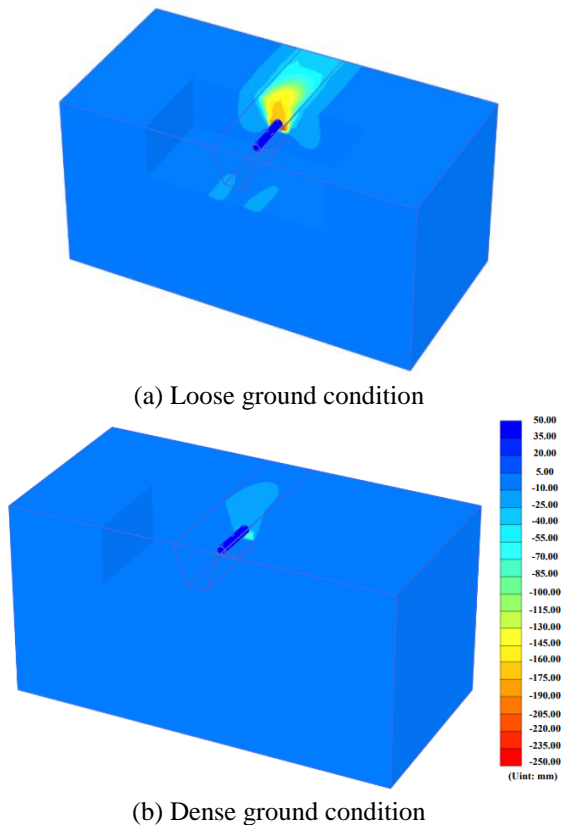


Fig. 21 Vertical displacement contours

cavity. In the case of the dense ground, there was only a settlement of 18 mm, which was approximately 12% of the settlement of the loose ground. In addition, the ground surface settlement gradually decreased with increasing

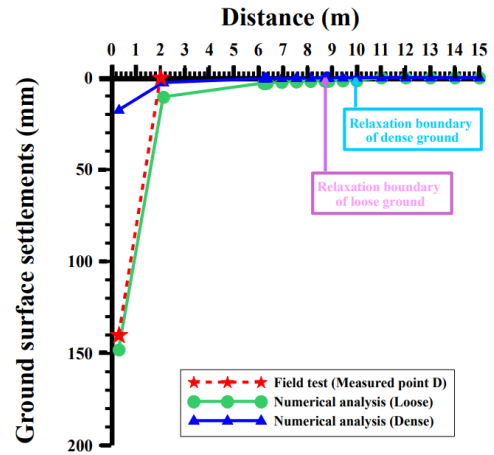


Fig. 22 Ground surface settlements

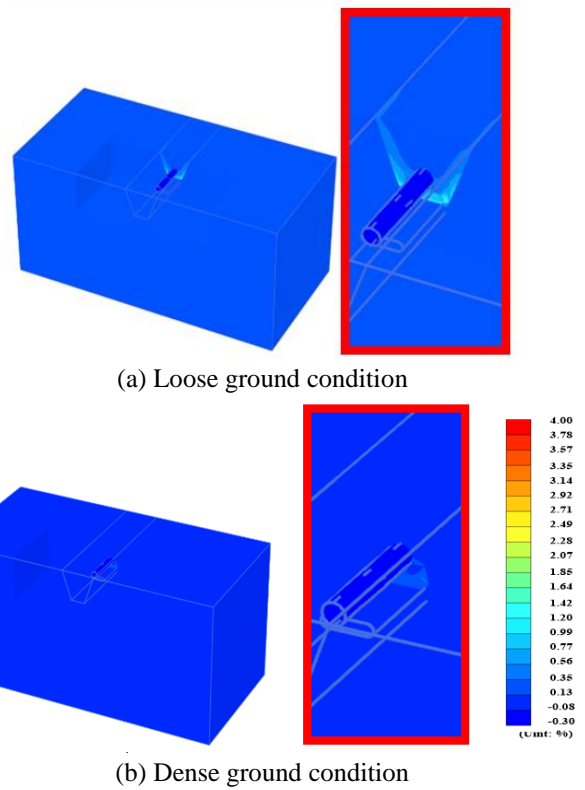


Fig. 23 Shear strain contours

distance from the upper part of the sewer pipe. The difference in ground surface settlement between the loose and dense ground was less than 10 mm at a position 2 m away from the upper part of the sewer pipe, which indicated that the impact on the surrounding ground was not significant (Fig. 22). The results of the shear strain can be seen in Fig. 23. In most geotechnical structures that are designed to restrict ground movements, the strains in the ground are usually quite small. The mean shear strains in the ground near the wall structure are 0.1%. Also, strain will decay to zero far from the structures (Atkinson 2007). In the case of the loose ground, the mean shear strains are about 0.1%, on the other hand, shear strains of 0.4% are generated in dense ground. Also, shear deformation occurred from the underground cavity to the ground surface along the

relaxation zone ($45^\circ + \Phi/2$). In the dense ground, shear deformation mainly occurred in the underground cavity and under the sewer pipe. Therefore, it can be concluded that the behaviour of the ground above the underground cavity was increasingly affected as the degree of compaction decreased.

5. Conclusions

In this study, field and laboratory tests were conducted to determine the behaviour of the ground caused by a cavity under a sewer pipe. The optimal compaction degree for preventing ground subsidence was predicted by comparing and analyzing the results of the field and laboratory tests. The results of this study can be summarized as follows.

- In this study, an underground cavity was simulated using an ice block to observe ground subsidence. In the field tests, position dependent settlements ranging from less than 10 mm to more than 140 mm were observed. It is believed that these differences were caused by the non-uniform site compaction. Therefore, uniform compaction is recommended when site compaction is performed.

- The compaction degree for each position of the site was estimated by way of field cone penetration and laboratory compaction tests. The results indicated that the estimated compaction degree of the area where a subsidence of more than 100 mm occurred was approximately 75-80% while that of the position where a subsidence of less than 100 mm observed was approximately 85-95%. Based on these results, it is believed that sudden subsidence can be prevented in case of an underground cavity when the compaction degree is more than 85%.

- The vertical displacement trend was similar to that of the total displacement. In the case of the loose ground, a maximum of 148 mm ground surface settlement occurred immediately above the sewer pipe. In the case of the dense ground, a displacement of 18 mm occurred, which was approximately 12% of the displacement of the loose ground. In addition, as the distance from the upper part of the sewer pipe increased, the amount of ground surface settlement gradually decreased. The difference in ground surface settlement between the loose and dense grounds was less than 10 mm at a position 2 m away from the upper part of the sewer pipe. These results appeared to be dependent on the cavity size, relaxation zone, and degree of compaction.

- In general, the mean shear strains in the ground near the wall structure are 0.1%. In loose sand, shear strains are generated about 0.1%, but, 0.4% in dense sand. So, authors recommend to construction in over 90% density.

- Shear deformation of the loose ground was observed between the underground cavity and ground surface along the relaxation zone ($45^\circ + \Phi/2$). In the case of the dense ground, shear deformation occurred in the underground cavity and below the sewer pipe, although it did not significantly affect the ground surface and the ground above the sewer pipe.

Acknowledgements

This research was supported by the Korea Agency for

Infrastructure Technology Advancement under the Ministry of Land, Infrastructure and Transport of the Korean government. (Project Number: 17SCIP-B108153-03) and Environment Ministry's Environment Policy Public Technology Development Project (Project Number: 2014000700006).

References

- Atkinson, J. (2007), *The Mechanics of Soils and Foundations*, Taylor & Francis, London, U.K.
- Cui, H., Hu, Q. and Song, M. (2017), "Spiral trajectory planning approach for underground cavity measurements based on laser scanning", *Measurement*, **110**, 166-175.
- Das, B.M. (2009), *Principles of Geotechnical Engineering*, Cengage Learning, San Francisco, California, U.S.A.
- Ham, T.G. (2009), "Method for the evaluation of strength parameter from the void ratio of decomposed granite soil after compaction using preconsolidation theory", *J. Kor. Geotech. Soc.*, **25**(6), 89-99.
- Im, J.C. (2015), Heartburn of Sinkhole, Magazine of the Korean Society of Civil Engineers, April.
- Kim, G.R., Kyung, D.H., Park D.G. and Lee, J.W. (2015), "CPT-based p-y analysis for mono-piles in sands under static and cyclic loading conditions", *Geomech. Eng.*, **9**(3), 313-328.
- Kim, J.Y., Kim, Y.S., Shin, Y.S., Han, H.J. and Jung, H.G. (2000), "Study on the applicability of high frequency seismic reflection method to the inspection of tunnel lining structures-Physical modeling approach", *J. Kor. Tunn. Undergr. Sp. Assoc.*, **2**(3), 37-45.
- Kuwano, R., Sato, M. and Sera, R. (2010), "Study on the detection of underground cavity and ground loosening for the prevention of ground cave-in accident", *Jap. Geotech. J.*, **5**(2), 219-229.
- Lambe, T.W. and Whitman, R.V. (1979), *Soil Mechanics*, John Wiley & Sons, Massachusetts, U.S.A.
- Lee, D.Y., Kim, D.M., Ryu, Y.S. and Han, J.G. (2015), "Development and application of backfill material for reducing ground subsidence", *J. Kor. Geosynth. Soc.*, **14**(4), 147-158.
- Lee, S., Kim, T.H. and Lee, J.H. (2007), *Method of Soil Test*, Goomibook, Seoul, Korea.
- Mouna, M., Ali, B., Khaled, R. and Nawel, A. (2017), "Analysis of load-settlement behaviour of shallow foundations in saturated clays based on CPT and DPT tests", *Geomech. Eng.*, **13**(1), 119-139.
- Oh, D.W., Ahn, H.Y. and Lee, Y. J. (2016), "A study for influence range of ground surface due to sewer fracture in various relative density of sand by laboratory model test", *J. Kor. Geotech. Soc.*, **32**(2), 19-30.
- Oh, D.W., Kong, S.M., Lee, D.Y., Yoo, Y.S. and Lee, Y.J. (2015), "Effects of reinforced pseudo-plastic backfill on the behavior of ground around cavity developed due to sewer leakage", *J. Kor. Geoenviron. Soc.*, **16**(12), 13-22.
- Park, I.J. and Park, S.H. (2014), "Analysis and countermeasures about sinkhole", *Mag. Kor. Soc. Hazard Mitig.*, **14**(5), 48-53.
- Perez, A.L., Nam, B.H., Alrowaimi, M., Chopra, M., Lee, S.J. and Youn, H. (2017), "Experimental study on sinkholes: Soil-groundwater behaviors under varied hydrogeological conditions", *J. Test. Eval.*, **45**(1), 208-219.
- Plaxis 3D. (2016), *Reference Manual*, Plaxis BV, Delft, The Netherlands.
- Ryu, H.H., Kim, G.Y., Lee, G.R., Lee, D.S. and Cho, G.C. (2015), "Exploration of underground utilities using method predicting an anomaly", *J. Kor. Tunn. Undergr. Sp. Assoc.*, **17**(3), 205-214.
- Sato, M. and Kuwano, R. (2015), "Influence of location of subsurface structures on development of underground cavities induced by internal erosion", *Soil. Found.*, **55**(4), 829-840.

- Tihansky, A.B. (1999), *Sinkholes, West-Central Florida, Land Subsidence in the United States*, Circular 1182, U.S. Geological Survey Circular, Reston, Virginia, U.S.A., 121-140.
- Zein, A.K.M. (2017), "Estimation of undrained shear strength of fine grained soils from cone penetration resistance", *Int. J. Geo-Eng.*, **8**(1), 1-13.

JS